Neuron, Vol. 27, 447–459, September, 2000, Copyright ©2000 by Cell Press

A Genetically Encoded Ratiometric Neurotechnique Indicator for Chloride: Capturing Chloride Transients in Cultured Hippocampal Neurons

Thomas Kuner† and George J. Augustine*
Department of Neurobiology
Duke University Medical Center
Durham, North Carolina 27710

Summary

We constructed a novel optical indicator for chloride ions by fusing the chloride-sensitive yellow fluorescent protein with the chloride-insensitive cyan fluorescent protein. The ratio of FRET-dependent emission of these fluorophores varied in proportion to the concentration of Cl^- and was used to measure intracellular chloride concentration ($[Cl^-]_i$) in cultured hippocampal neurons. $[Cl^-]_i$ decreased during neuronal development, consistent with the shift from excitation to inhibition during maturation of GABAergic synapses. Focal activation of $GABA_A$ receptors caused large changes in $[Cl^-]_i$ that could underlie use-dependent depression of GABA-dependent synaptic transmission. GABA-induced changes in somatic $[Cl^-]_i$ spread into dendrites, suggesting that $[Cl^-]_i$ can signal the location of synaptic activity. This genetically encoded indicator will permit new approaches ranging from high-throughput drug screening to direct recordings of synaptic Cl^- signals in vivo.

Introduction

Chloride ions subserve many physiological functions, including regulation of cell volume, intracellular pH, fluid secretion, and stabilization of the resting membrane potential. In mature neurons, Cl^- is the main mediator of synaptic inhibition because both GABA and glycine activate Cl^- selective ion channels to generate postsynaptic electrical signals. Developmental regulation of intracellular Cl^- concentration ($[Cl^-]_i$) apparently determines whether GABAergic synapses excite or inhibit their postsynaptic target (Cherubini et al., 1991; Rivera et al., 1999). A switch between inhibition and excitation also occurs during sustained activation of GABA receptors (Barker and Ransom, 1978; Alger and Nicoll, 1979), due to an accumulation of Cl^- and subsequent local collapse of the Cl^- gradient (Staley et al., 1995; Staley and Proctor, 1999). Other dynamic changes in $[Cl^-]_i$ may regulate signal transduction in olfactory neurons (Nakamura et al., 1997), astrocytes (Bekar and Walz, 1999), and hypothalamic neurons (Wagner et al., 1997). Several human diseases have been linked to dysfunctional Cl^- homeostasis, including cystic fibrosis (Kerem et al., 1989), myotonia congenita (Koch et al., 1992), inherited hypercalciuric nephrolithiasis (Lloyd et al., 1996), Bartter syndrome (Simon et al., 1996), and hyperekplexia/startle disease (Shiang et al., 1993).

Despite the physiological importance of $[Cl^-]_i$, only a few studies have reported direct measurements of $[Cl^-]_i$ in acutely isolated ganglia (Ascher et al., 1976; Ballanyi and Grafe, 1985), neuromuscular preparations (Kaila et al., 1992), dissociated neurons (Engblom et al., 1991; Inoue et al., 1991; Hara et al., 1992; Dallwig et al., 1999), or brain slices (Schwartz and Yu, 1995; Frech et al., 1999; Inglefield and Schwartz-Bloom, 1999). This is largely due to limitations in the experimental approaches available to study $[Cl^-]_i$. For example, Cl^--selective electrodes (Thomas, 1978) can only be used inside large cells and offer limited selectivity. Radioactive tracers (Harris and Allan, 1985; Schwartz et al., 1985) are not very sensitive, have limited time resolution, and typically report Cl^- fluxes rather than $[Cl^-]_i$. Only optical methods offer the potential for spatially resolved measurements of $[Cl^-]_i$. Cl^- indicator dyes adequate for detecting changes in Cl^- have been developed, but determining absolute Cl^- concentrations remains difficult (summarized in Inglefield and Schwartz-Bloom, 1999) despite recent synthesis of a ratiometric Cl^- indicator (Jayaraman et al., 1999). These organic Cl^- indicators cannot take advantage of genetic methods of targeting and need to be delivered into cells by potentially disruptive methods. In addition, organic dyes can be toxic and often are poorly retained within cells.

While using fluorescence resonance energy transfer (FRET) to study protein–protein interactions, we observed that the efficiency of FRET between the cyan fluorescent protein (CFP) and yellow fluorescent protein (YFP) was sensitive to Cl^-. Here, we demonstate that a fusion protein containing these two fluorophores can be used as a ratiometric, targetable, and genetically encoded Cl^- indicator. Further, we demonstrate the utility of this protein as a reporter of $[Cl^-]_i$ in cultured hippocampal neurons. We show that $[Cl^-]_i$ decreases during neural development, dropping from essentially extracellular concentrations at embryonic day 18 to an order of magnitude lower by postnatal day 14. Finally, we demonstrate that $GABA_A$ receptor–mediated Cl^- fluxes can substantially change $[Cl^-]_i$ in the soma of a neuron and can spread into the dendrites. Such transients may affect the regional balance of dendritic inhibition and excitation, suggesting a possible functional role for Cl^- transients in intracellular signaling. The favorable functional attributes of the indicator, combined with the possibility of genetically targeted expression, will permit novel experimental analyses of the physiological functions of Cl^- in cells, tissues, and animals.

Results

The ratiometric indicator is based on the coupling of CFP with YFP via a flexible peptide linker (Figure 1A). When expressed in bacteria, this construct gave rise to a ~59 kDa fusion protein that could be purified via its histidine tag (Figure 1B). Illumination of recombinant

*To whom correspondence should be addressed (e-mail: georgea@neuro.duke.edu).
†Present address: Max-Planck-Institute for Medical Research, Abteilung Zellphysiologie, Jahnstrasse 29, 69126 Heidelberg, Germany.

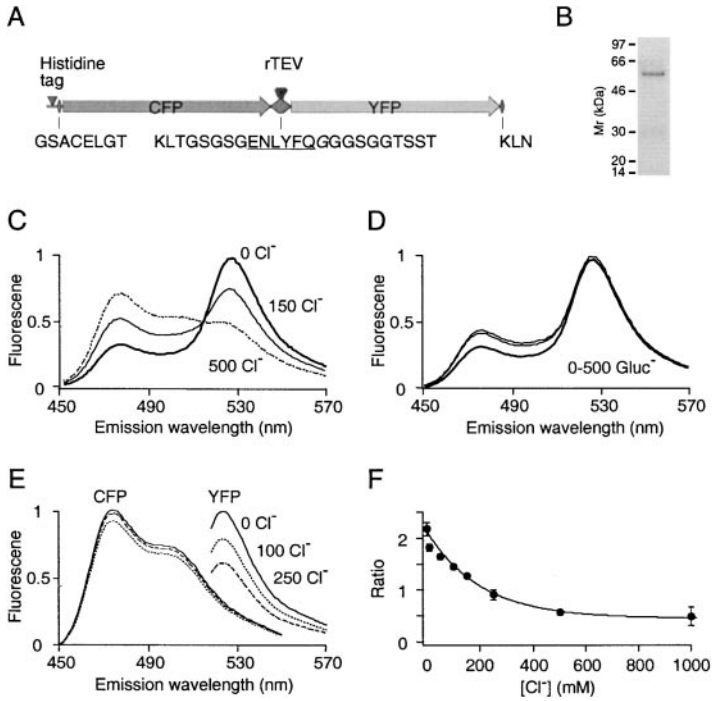

Figure 1. Design and Basic Properties of Clomeleon

(A) Structure of Clomeleon. The sequence recognized by the rTEV protease is underlined.

(B) Purified recombinant Clomeleon protein (molecular weight ~59 kDa) analyzed on a SDS–PAGE gel stained with Coomassie blue. The faint band at 30 kDa is likely to represent individual CFP and YFP molecules generated by hydrolytic cleavage of the linker.

(C) Emission spectra of Clomeleon in the presence of different [Cl^-]. In all cases, the recombinant protein was excited at 434 nm and the emission spectra were normalized to their peaks at 527 nm.

(D) Lack of effect of gluconate on Clomeleon emission spectra (434 nm excitation).

(E) Emission spectra of recombinant CFP and YFP excited at 434 nm and 510 nm, respectively. Fluorescence signals are normalized to the peak of the spectra determined in the absence of Cl^-.

(F) The relationship between fluorescence emission ratio (527 nm/485 nm) and [Cl^-]. Points indicate mean ± SEM (n = 3, same batch of protein) and the line is an exponential function fit to the data.

protein at 434 nm resulted in emission of the CFP fluorophore at 485 nm and emission of the YFP fluorophore at 527 nm (Figure 1C, thick line). Cleavage of the peptide linker with rTEV protease resulted in an increase of the donor fluorescence at 485 nm and a loss of the acceptor fluorescence at 527 nm (data not shown), demonstrating that emission at 527 nm was induced via FRET from CFP to YFP.

The ratio of fluorescence emission of the YFP acceptor to that of the CFP donor ($R = F_{527}/F_{485}$) depended on the concentration of potassium chloride in the solution (Figure 1C). This ratio decreased from 2.45 ± 0.37 (mean ± SEM, three different protein preparations) in water to 0.55 ± 0.06 in the presence of 500 mM potassium chloride (Figure 1C, stippled line). In the presence of equivalent concentrations of potassium gluconate, the ratios remained largely unchanged (Figure 1D), indicating that the changes in R produced by potassium chloride are mediated by Cl^-. This Cl^--induced decrease in the apparent FRET efficiency is due to a selective quenching of YFP fluorescence: YFP fluorescence was sensitive to Cl^-, while Cl^- had no significant effect on the fluorescence emitted by CFP (Figure 1E). Increasing [Cl^-] produced a monotonic reduction in R (Figure 1F). Half-maximal reduction in R occurred at ~160 mM, and R was saturated at [Cl^-] higher than 500 mM. We have named this Cl^- indicator Clomeleon, an allusion to the FRET-based, genetically encoded calcium indicator Cameleon (Miyawaki et al., 1997).

Although Clomeleon is insensitive to gluconate, we wanted to know whether it was sensitive to other anions. Halides strongly inhibited Clomeleon fluorescence, with Cl^- the least potent and F^- the most potent. The affinity of Clomeleon for these halides varied in the sequence $F^- > I^- > Br^- > Cl^-$ (Figure 2A). Halide titration curves were fit with the Hill equation and yielded Hill coefficients close to 1 (Table 1), suggesting the presence of a single halide interaction site on each Clomeleon molecule. Among the other anions that were tested, 150 mM NO_3^- strongly inhibited Clomeleon fluorescence but is unlikely to be present within cells at such a high concentration (Table 1). The other anions had only small effects on R at this supraphysiological concentration (Table 1). Clomeleon was insensitive to the cation listed in Table 1, except for Cd^{2+}, which potentiated the fluorescence ratio 2.5-fold. Hence, among these ions, only Cl^- is likely to interact with Clomeleon inside cells.

Because the fluorescence of YFP is known to be strongly dependent on pH (Tsien, 1998), we investigated whether H^+ influences the interaction of Clomeleon with Cl^-. The relationship between Clomeleon fluorescence and [Cl^-] was measured at different pH values over the physiologically relevant range of 7.0–7.8. Cl^- was more effective in quenching Clomeleon fluorescence at high concentrations of H^+ (Figure 2B). The parallel shift of the Cl^- titration curves suggests that H^+ and Cl^- interact allosterically to produce such a synergistic effect. Replotting these data as a function of pH emphasizes that the sensitivity of Clomeleon to H^+ depends upon [Cl^-], being low at 10 mM [Cl^-] and high at 150 mM [Cl^-] (Figure 2C). The influence of protons on the Cl^- sensitivity of Clomeleon caused the IC_{50} for Cl^- to shift 10-fold for a pH change of one unit (Figure 2D). As a result, if Clomeleon were calibrated at pH 7.4, changing the pH by 0.2 units (without recalibrating the indicator) would cause the apparent [Cl^-] to change only a few millimolar for [Cl^-] less than 50 mM but would result in large deviations at 150 mM [Cl^-] (Figure 2E). Thus, the effects of pH on Clomeleon fluorescence are especially prominent when measuring [Cl^-] greater than 50 mM. The errors introduced by large pH shifts, without recalibrating the indicator, remains below 20% at [Cl^-] below 25 mM but

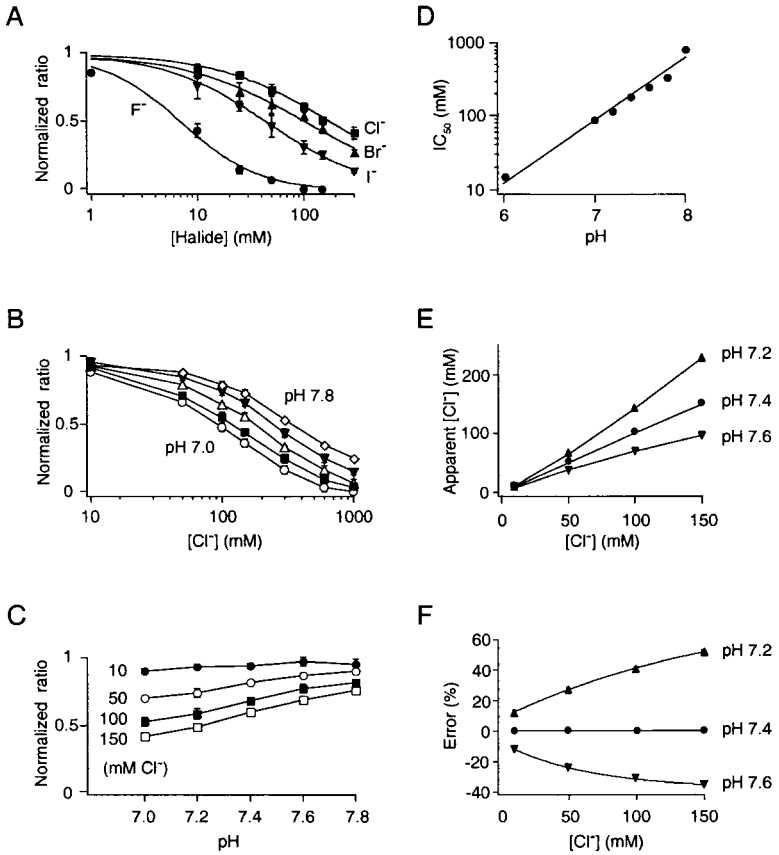

Figure 2. Ion Sensitivity of Chlomeleon

(A) Titration curves for recombinant Clomeleon protein in the presence of various halide ions. Symbols designate mean ± SEM of three to five independent experiments using two different batches of protein and two different sets of solutions. The lines are fits to the Hill equation with parameters listed in Table 1. The ratios were normalized for each experiment to R_{max} obtained in 150 mM potassium gluconate solution and R_{min} obtained in 150 mM KF solution.

(B) Parallel shifts of the Cl^- titration curves at various H^+ concentrations. Each data point represents the mean ± SEM of three experiments. Data normalization as in (A).

(C) Influence of Cl^- on H^+ sensitivity of Clomeleon fluorescence ratio. From data shown in (B).

(D) Relationship between pH and IC_{50} for Cl^- quenching of Clomeleon.

(E) Shifts in the readout of $[Cl^-]$ by Clomeleon if the indicator was calibrated at pH 7.4 but used at the indicated pH values.

(F) Relative error in the readout of $[Cl^-]$ at pH 7.2 and pH 7.6 for the case where Clomeleon is calibrated at pH 7.4. Calculated from data shown in (E).

approach 50% for decreases in pH at $[Cl^-]$ of 150 mM or more (Figure 2F).

Clomeleon Reports Cl^- Concentration in Cultured Hippocampal Neurons

The in vitro data presented above suggests that Clomeleon should be suitable as an indicator of intracellular Cl^- concentration ($[Cl^-]_i$) in living cells. To examine this possibility, we expressed Clomeleon in cultured hippocampal neurons by electroporation (Teruel et al., 1999) of an expression plasmid carrying the coding region of Clomeleon under the control of a CMV promoter. Expression of Clomeleon was routinely observed 24 hr after electroporation and was maintained at high levels for at least 5 days. Neurons expressing Clomeleon exhibited homogeneous fluorescence throughout each cell, including the soma, nucleus, proximal, and distal dendrites (Figure 3A). Therefore, measurements of Clomeleon fluorescence are likely to reflect the average $[Cl^-]_i$ in each of these compartments.

To calibrate the fluorescence of Clomeleon within these neurons, R was measured while using a patch pipette to manipulate the cytoplasmic concentration of anions (Figure 3B). A nominally Cl^--free solution containing 150 mM gluconate was used to determine the maximal emission ratio for Clomeleon (R_{max}), whereas a solution containing a saturating concentration (150 mM) of F^- defined the minimal emission ratio (R_{min}). The relationship between R and intermediate values of $[Cl^-]_i$ was then determined (Figure 3C). This relationship could be described as $[Cl^-] = K_d' \bullet (R_{max} - R)/(R - R_{min})$, with $R_{max} = 2.39$, $R_{min} = 0.49$, and $K_d' = 87$ mM. This calibration curve could then be used to convert R values measured in hippocampal neurons into $[Cl^-]_i$.

Clomeleon Captures $[Cl^-]_i$ Switch during Neuronal Development

In embryonic neurons, GABA elicits depolarizing currents, whereas in adult neurons, these currents are hyperpolarizing (Cherubini et al., 1991). This developmental switch is paralleled by changes in $[Cl^-]_i$, created by the regulated expression of Cl^- transporters (Rivera et al., 1999). We sought to use Clomeleon to directly measure $[Cl^-]_i$ during the development of cultured hippocampal neurons. Cells maintained in culture for 2–4 days were used to assess $[Cl^-]_i$ at developmental stages embryonic day 18 (E18) to postnatal day 4 (P4). For example, E20 includes measurements from neurons and glial cells prepared from rats that were at developmental stages E16 and E18. Measurements for later stages, P8–P14, were made on cells maintained in culture for 4–10 days. For each stage, 5–15 cells were selected randomly, and $[Cl^-]_i$ was calculated from R measured at the soma of each cell. $[Cl^-]_i$ in glial cells was quite low early in development and did not change significantly over the first postnatal week (Figure 4, open symbols). In contrast, neuronal $[Cl^-]_i$ was much higher (~140 mM) at E18, the earliest embryonic stage considered (Figure 4, filled symbols). $[Cl^-]_i$ decreased to about 60 mM at P0 and then further decreased to about 20 mM

Table 1. Halide Sensitivity and Ionic Selectivity of Clomeleon

Halide	IC_{50} (mM)	Hill Coefficient	Number of Determinations
F^-	5.9 ± 2.4	1.25 ± 0.09	(3)
Cl^-	167 ± 13	0.87 ± 0.07	(5)
Br^-	111 ± 21	0.82 ± 0.09	(3)
I^-	46 ± 14	0.90 ± 0.07	(3)
Anion[a]		Ratio compared to H_2O	
H_2O		1.00	
Gluconate		0.87 ± 0.02	
Glutamate		0.83 ± 0.01	
HCO_3^-		0.74 ± 0.04	
ATP^{2-}		0.73 ± 0.06	
Methylsulfate		0.71 ± 0.05	
PO_4^{2-}		0.68 ± 0.01	
SO_4^{2-}		0.68 ± 0.04	
Cl^-		0.58 ± 0.02	
NO_3^-		0.42 ± 0.05	
Cation[b]		Ratio Compared to KCl Solution	
K^+		1.00	
Na^+		0.99 ± 0.01	
Cs^+		0.95 ± 0.02	
Li^+		1.02 ± 0.03	
Ca^{2+}		0.92 ± 0.03	
Mg^{2+}		0.94 ± 0.01	
Mn^{2+}		0.93 ± 0.03	
Sr^{2+}		0.92 ± 0.04	
Ba^{2+}		0.94 ± 0.05	
Co^{2+}		0.93 ± 0.03	
Cd^{2+}		2.57 ± 0.42	

All values mean ± SEM (n = 3) unless stated otherwise.
[a] All solutions contained 150 mM anion, except for ATP^{2-} (10 mM), plus 10 mM HEPES pH 7.4.
[b] All solutions contained 160 mM Cl^-, either 160 mM monovalent cations or 10 mM divalent cations, plus 10 mM HEPES pH 7.4.

at P14. This temporal profile of $[Cl^-]_i$ is consistent with the developmental switch in GABA-mediated synaptic transmission reported in neurons from several brain regions (Cherubini et al., 1991). These results demonstrate that Clomeleon is capable of reporting resting $[Cl^-]_i$ in living cells.

GABA Activated Cl^- Transients Measured by Clomeleon

Cl^--sensitive microelectrodes have been used to resolve transient changes in $[Cl^-]_i$ resulting from activation of GABA receptors (Ballanyi and Grafe, 1985; Kaila et al., 1992). We next asked whether Clomeleon could detect such signals in cultured hippocampal neurons. For this purpose, brief pulses of GABA were applied, via pressure, from a micropipette positioned within 10–30 μm of the soma of individual neurons. Whole-cell patch-clamp recordings were used to measure electrical currents elicited by such focal applications of GABA and fluorescence signals were simultaneously recorded from the soma of the neurons.

An example of the simultaneous measurement of GABA-induced Cl^- currents and changes in $[Cl^-]_i$ is shown in Figure 5A. In this experiment, the cell was held at a membrane potential of +60 mV to create a large driving force for Cl^- influx. When GABA was applied to the neuron (triangle), a large outward Cl^- current developed (continuous line), causing intracellular Cl^- concentration to increase from its resting value of 15 mM up to 85 mM at the peak of the response (filled circles). The rise in $[Cl^-]_i$ occurred with a short delay of ~1 s and reached baseline ~10 s after the Cl^- current ceased. The slowed time course of the change in intracellular Cl^- concentration, in comparison to the current signal, is likely to be limited by several factors, including the kinetics of Cl^- binding by Clomeleon and the rate at which Cl^- is removed from the cell.

The experiment shown in Figure 5A was repeated in the same cell, except the membrane potential was hyperpolarized to −80 mV to create electrochemical conditions that produce an efflux of Cl^-. In this case, GABA application elicited an inward Cl^- current (Figure 5B). This current was briefer in duration than at depolarized potentials, at least in part due to the voltage-dependent gating behavior of $GABA_A$ receptor channels (Bormann et al., 1987). The GABA-induced efflux of Cl^- led to a decrease in $[Cl^-]_i$ that again was slightly delayed in onset relative to the GABA-induced Cl^- current and returned to baseline within 15 s after the end of this current.

The magnitude of the changes in $[Cl^-]_i$ reported by Clomeleon correlated with the size of the measured Cl^- currents. The relationship between the amplitude of outward Cl^- currents and the resultant rises in $[Cl^-]_i$ is summarized in Figure 5C. Currents as small as 100 pA produced detectable changes in $[Cl^-]_i$ that ranged from 10–20 mM, depending on the size of the neuron, while currents larger than 500 pA generated changes in $[Cl^-]_i$ that were as large as 90 mM. This correlation suggests that the measured changes in the fluorescence of Clomeleon faithfully reflect changes in $[Cl^-]_i$. As an additional way to validate our measurements of $[Cl^-]_i$, we

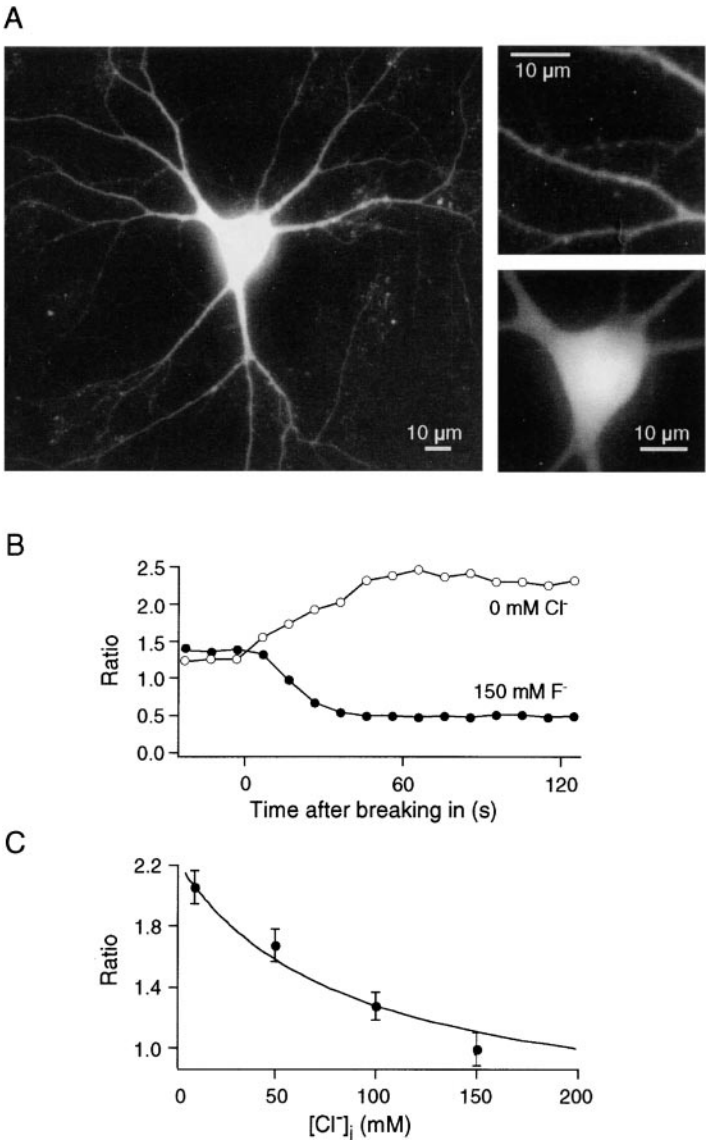

Figure 3. Expression of Clomeleon in Cultured Hippocampal Neurons and Calibration of $[Cl^-]_i$

(A) Images of a hippocampal neuron expressing Clomeleon; right panel shows magnified regions of the same neuron.

(B) Diffusional exchange of $[Cl^-]_i$ with patch pipette solutions to determine R_{min} and R_{max}.

(C) Fluorescence ratios as a function of neuronal $[Cl^-]_i$. Symbols represent the mean ± SEM of five to eight independent experiments. The line was calculated from the equation $[Cl^-] = 87\ mM \bullet (2.39 - R)/(R - 0.49)$.

used the fluxes of Cl^-, determined from the recorded Cl^- currents, to predict the resultant change in $[Cl^-]_i$. Figure 5D illustrates an example of this prediction, taken from the experiment shown in Figure 5B. The amount of Cl^- leaving the cell was determined by integrating the current elicited by GABA and was converted into a change in $[Cl^-]_i$ by dividing by the Faraday constant and the cell's volume of 1 pl (estimated from the dimensions of the soma). The efflux of 30 fmoles Cl^- was predicted to create a drop in $[Cl^-]_i$ by about 30 mM (Figure 5D, open circles) in remarkable agreement with the peak change in $[Cl^-]_i$ measured in this experiment (Figure 5D, filled circles). At later times, the $[Cl^-]_i$ reported by Clomeleon deviated from this prediction due to removal of Cl^- from the cell. This correspondence shows the ability of Clomeleon to measure $[Cl^-]_i$ reliably.

Because Clomeleon is sensitive to pH (Figure 2), and changes in $[Cl^-]_i$ can affect intracellular pH (Hoffmann and Simonsen, 1989), it is possible that some of the signal reported by Clomeleon following GABA application could be due to changes in pH rather than $[Cl^-]_i$. To consider this possibility, we used the ratiometric pH indicator BCECF (Rink et al., 1982) to measure intracellular pH during GABA application (Figure 5E). In eight experiments, GABA-induced Cl^- currents similar in magnitude to the examples shown above resulted in an average decrease of the intracellular pH by 0.016 ± 0.002 units. From the relationship shown in Figure 2E, such a change in pH would affect our estimate of $[Cl^-]_i$ by no more than 0.17 mM. This is very small in comparison to the 40–60 mM rise in $[Cl^-]_i$ that would be expected following such GABA-induced currents (Figure 5C). Hence, the Clomeleon fluorescence signal we have measured during GABA application essentially reflects only changes in $[Cl^-]_i$.

Cl^- Signaling in Dendrites

Localized Cl^- fluxes such as those occurring during GABA action could modify $[Cl^-]_i$ throughout the neuron. To examine this possibility, we looked at the spatial spread of GABA-induced changes in $[Cl^-]_i$ within individual pyramidal neurons kept in culture for 12–16 days.

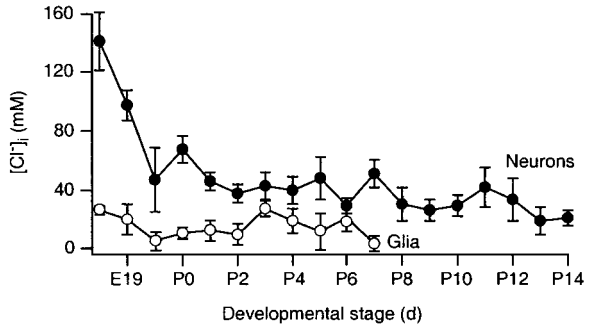

Figure 4. Developmental Time Course of Intracellular Cl^- Concentration

Symbols represent the mean ± SEM of 5–15 measurements on neurons and 3–5 measurements on glia.

We first examined the possibility of gradients in resting $[Cl^-]_i$ within these neurons. The average somatic $[Cl^-]_i$ was 7.9 ± 2 mM (n = 9), $[Cl^-]_i$ was 7.0 ± 3 mM (n = 9) in proximal dendrites up to 50 μm away from the somata, and $[Cl^-]_i$ was 12.2 ± 4 mM (n = 9) at distances between 50 and 150 μm from the somata. However, $[Cl^-]_i$ was significantly (ANOVA, Neuman-Keuls test, $p < 0.01$) increased to 25 ± 5.5 mM (n = 7) in peripheral dendrites >250 μm from the soma. This measurement of $[Cl^-]_i$ is unlikely to reflect a dendritic pH gradient rather than a Cl^- gradient because pH would have to be at an improbable value of ~6.4 to account for the lower R measured in the distal dendrites (Figure 2E).

We next asked whether focal application of GABA onto the soma of a neuron could alter $[Cl^-]_i$ in other regions of the neuron. The arrangement of these experiments is shown in the left panel of Figure 6. To restrict the application of GABA to the cell body of the neuron, an application pipette containing 1 mM GABA was placed close to the soma and a suction pipette was placed nearby to aspirate the GABA solution before it could diffuse to other parts of the cell (Bekkers et al., 1990). Moving the application pipette 25 μm away from the soma resulted in a drop of the current responses to <10% of the value recorded when the soma was fully exposed to the solution stream, indicating that GABA application was restricted to a small volume between the tips of the application and suction pipettes. GABA was applied locally onto the soma, while $[Cl^-]_i$ was recorded serially at three regions along a single primary dendrite, starting with the most distal region. Cl^- influx through somatic $GABA_A$ receptor channels led to a large outward current, measured by a patch pipette (Figure 6, right panel). In addition to elevating $[Cl^-]_i$ within the cell body, the GABA-induced influx of Cl^- also increased $[Cl^-]_i$ in the dendrite. In the cell shown in Figure 6 (right panel), $[Cl^-]_i$ increased by ~35 mM within the soma, by ~30 mM close to the soma, and by ~10 mM at a distance of 140 μm. The timing of the peaks of these responses correlated with the distance from the soma: at the most distant site (140 μm), the maximal increase in $[Cl^-]_i$ was reached in 7 s, after 4 s at an intermediate distance (70 μm), and within 2.5 s near the soma (10 μm). These values are consistent with Cl^- having an intracellular diffusion coefficient of $\sim 2 \times 10^{-5}$ cm^2 s^{-1}, close to the diffusion coefficient of Cl^- in free solution. The decay of the Cl^- transients also correlated with the distance from the soma, with $[Cl^-]_i$ returning to baseline slowest in the distant dendritic region. Thus, activation of somatic $GABA_A$ receptor channels can create dendritic Cl^- transients that outlast the initial current response. These changes in $[Cl^-]_i$ are of sufficient magnitude to transiently shift the equilibrium potential for chloride (E_{Cl}); for example, a rise in $[Cl^-]_i$ from 10 mM to 30 mM will shift E_{Cl} from −68 mV to −33 mV. For a neuron with a resting potential of −60 mV, such a change in E_{Cl} will cause a GABAergic synaptic input to switch from inhibitory to excitatory. Thus, we conclude that activation of GABA receptors can produce shifts in E_{Cl} that can affect the magnitude and polarity of Cl^--dependent synaptic transmission. Further, these shifts can spread beyond the site of Cl^- influx into nearby regions of the neuron.

Discussion

Here, we introduce Clomeleon, a genetically encodable, ratiometric Cl^- indicator and demonstrate its ability to measure intracellular Cl^- concentrations in cultured hippocampal neurons. Cl^- quenches the YFP moiety of Clomeleon, resulting in a decrease in FRET efficiency that is measured as a decrease in the ratio of fluorescence emission between the YFP acceptor and CFP donor fluorophores. Clomeleon exhibited an IC_{50} for Cl^- of 167 mM, which puts the dynamic range of this indicator well within the range of physiological shifts in $[Cl^-]_i$. While Clomeleon is sensitive to halides other than Cl^-, physiologically relevant anions such as PO_4^{2-}, HCO_3^-, and ATP^{2-} had only small effects at concentrations much higher than those found in cytoplasm. Apart from Cd^{2+} and H^+, none of the cations tested affected Clomeleon fluorescence. Cd^{2+} caused a strong potentiation of YFP fluorescence at high concentrations (10 mM), whereas increasing concentrations of H^+ enhanced the sensitivity of Clomeleon for Cl^-. However, even large shifts in pH caused relatively small changes in the apparent affinity of Clomeleon for Cl^- at $[Cl^-]$ below 50 mM (Figure 2). The properties described here make Clomeleon well-suited as a tool to measure $[Cl^-]_i$ in a wide variety of cells.

Clomeleon as a Ratiometric Cl^- Indicator

The ability of Clomeleon to serve as a ratiometric indicator is based on FRET between the fluorophores of CFP and YFP. The fact that CFP and YFP are differentially sensitive to Cl^- causes the ratio of fluorescence emission to change in response to $[Cl^-]$. Quenching of YFP by Cl^- has been reported independently (Wachter and Remington, 1999), and a variant of YFP, YFP-H148Q, has been proposed as a genetically encoded indicator for $[Cl^-]$ (Jayaraman et al., 2000). Although Clomeleon and YFP-H148Q share the same mechanism of Cl^- sensitivity, YFP-H148Q does not permit ratiometric measurements. A second chloride-dependent peak occurs around 400 nm in the absorbance spectrum of YFPs (e.g., Figure 1C; Jayaraman et al., 2000). This peak cannot be used for ratiometric imaging because it is prominent only under conditions of low pH and does not result in the emission of fluorescence (data not shown). Thus, our work harnesses quenching of YFP to produce a ratiometric indicator by fusing it with the Cl^--insensitive

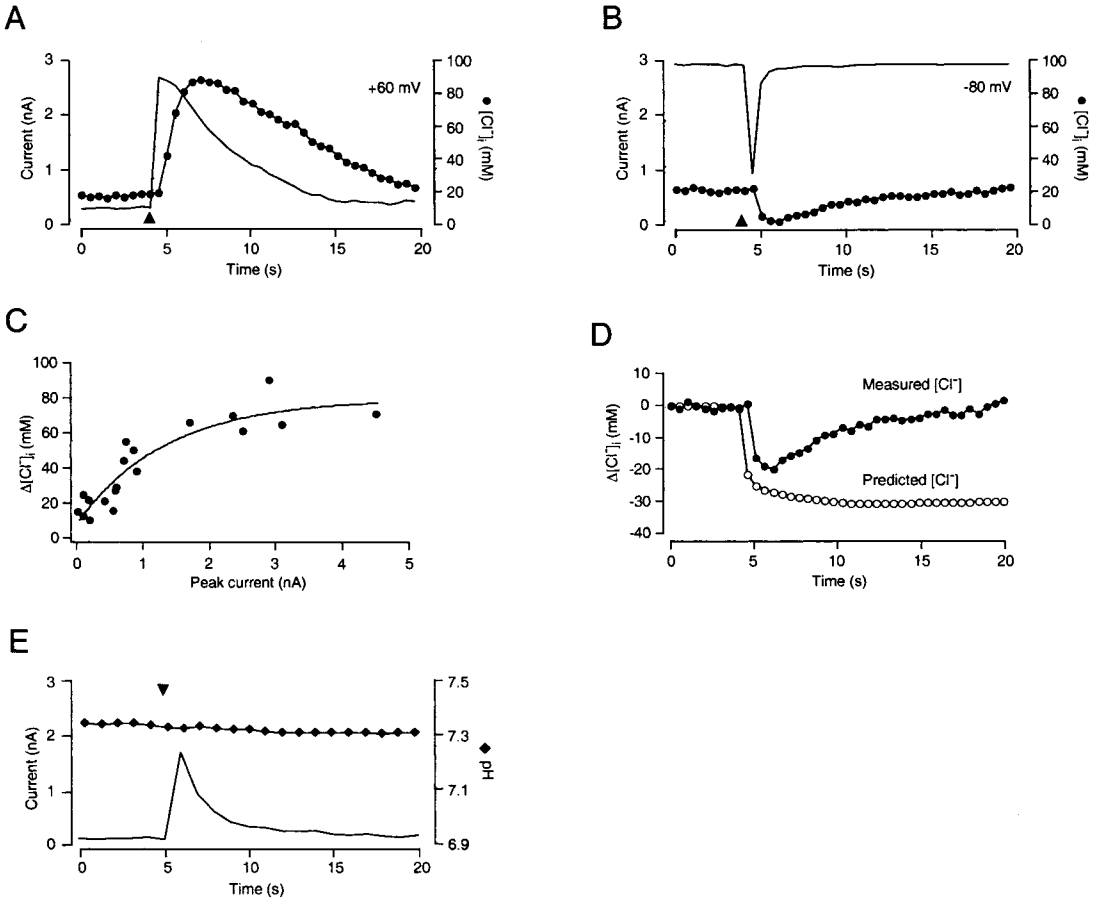

Figure 5. GABA Mediated Cl^- Currents and Concurrent Changes in $[Cl^-]_i$

(A) GABA-induced current elicited at a membrane potential of +60 mV (thin line). A 25 ms long pulse of 1 mM GABA was applied at t = 4 s (triangle). Cl^- concentrations (filled circles) were calculated using the calibration curve shown in Figure 3C.

(B) GABA responses detected at a membrane potential of −80 mV.

(C) Relationship between the peak amplitudes of GABA-induced currents and changes in $[Cl^-]_i$. Each symbol was obtained from an independent experiment.

(D) Change in $[Cl^-]_i$ predicted from the integral of the GABA-induced current shown in (B) compared with the measured change in $[Cl^-]_i$.

(E) Measurement of pH (diamonds) in a hippocampal neuron during the GABA-induced current response (thin line) elicited at a membrane potential of +30 mV.

CFP. The ratiometric capabilities of Clomeleon allow optical measurements that are minimally influenced by the thickness of the specimen, intensity of the excitation light, or concentration of the indicator (Bright et al., 1989). This, in turn, makes it possible to accurately determine absolute Cl^- concentrations even in cells with complicated geometry, such as neurons.

Clomeleon has several other features that are advantageous for measuring $[Cl^-]_i$. (1) This indicator utilizes excitation light in the visible range, thereby avoiding strong autofluorescence and phototoxicity typically occurring with near-UV illumination. (2) The high absorbances and quantum yields of CFP and YFP establish a good signal-to-noise ratio at low indicator concentrations. Because the concentration of the indicator is only a few micromolar—about 10^3–10^5 times lower than the concentration of Cl^-—it is easy to avoid the sort of buffering effects that plague fluorescence measurements of intracellular calcium (Neher and Augustine, 1992). (3) Clomeleon is not affected by other physiologically relevant anions, including the somewhat exotic anions (such as gluconate) sometimes used in electrophysiological recordings. (4) Loading of Clomeleon into cultured cells, tissues, and animals can be achieved by conventional methods of gene transfer, as well as by microinjection. (5) The relatively high molecular mass of Clomeleon (~59 kDa) retards diffusion of the indicator, preventing the indicator from rapidly collapsing spatial gradients of Cl^-. This slow diffusion of Clomeleon also retards the wash-out of Clomeleon from cytoplasm during whole-cell patch-clamp recordings, such as those shown in Figures 5 and 6. (In neurons that are imaged without simultaneous electrophysiological recordings, indicator levels will remain constant over hours.) (6) The fact that Clomeleon is a genetically encoded indicator should allow it to be targeted to specific cell types, by cell-specific promoters, or to defined cellular compartments by fusion to short sequence tags (e.g., palmitoylation) or proteins of known location.

While a clear advance over previous Cl^--sensitive indicators, Clomeleon still has some potential limitations. One is that Clomeleon is sensitive to pH, which influ-

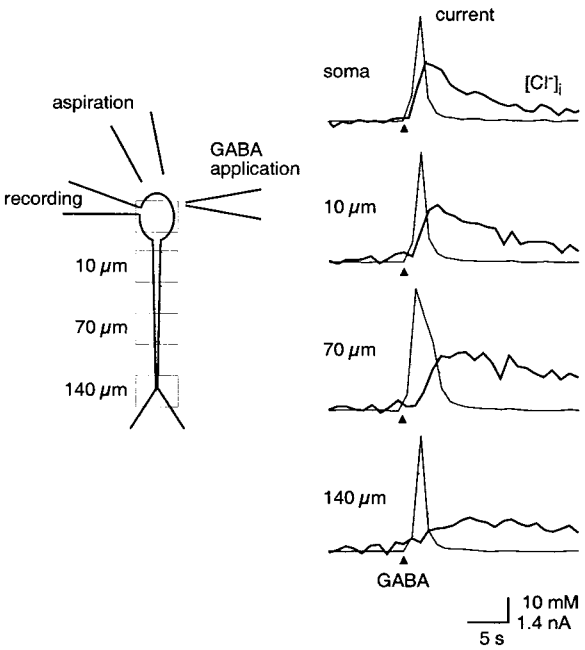

Figure 6. Dendritic Cl^- Signaling

Left: Diagram of arrangement for locally applying GABA onto a hippocampal neuron. Right: Cl^- transients (thick lines) recorded from the regions marked on the left panel. GABA (1 mM GABA, 0.5 s) was focally applied onto the soma of the neuron (triangles) at a holding potential of 10 mV and elicited the Cl^- currents shown by thin lines.

ences the affinity of the indicator for Cl^-. All genetically encoded indicators are at least somewhat influenced by pH because GFP is intrinsically proton sensitive, like most other proteins. The pH sensitivity of Clomeleon is similar to most ion-sensitive GFP derivatives (Tsien, 1998) and is significantly better than YFP-H148Q (Jayaraman et al., 2000), which has a pK_a very close to physiological pH (Table 2). Systematic mutagenesis of Clomeleon should further improve its pH dependence to yield an indicator with even more favorable properties. In practice, intracellular pH is tightly regulated in cells (Amos and Richards, 1996) so that changes in intracellular pH usually will be too small to significantly affect Clomeleon fluorescence. Even relatively large changes in pH (e.g., 0.2 unit changes from pH 7.4) would cause almost no deviations when recording small $[Cl^-]$, whereas at concentrations >50 mM, such changes in pH can significantly affect indicator readout (Figures 2E and 2F). Larger pH changes would produce larger apparent changes in $[Cl^-]$, especially at high $[Cl^-]$, but are unlikely to occur in healthy neurons. It is important to emphasize that the influence of pH is most prevalent in experimental conditions where pH is not directly controlled, such as when measuring $[Cl^-]$ in vivo. But when whole-cell patch pipettes are used, as in the experiments shown in Figures 5 and 6, intracellular pH can be tightly clamped by the pH buffer of the internal solution. In all applications, it will be important to calibrate Clomeleon at the physiological pH of the cell type under investigation.

Clomeleon also has other, less significant limitations. One is that the time course of its response to $[Cl^-]$ changes is somewhat slow. For example, in the experiments shown in Figures 5 and 6, measured rises in $[Cl^-]_i$ lagged behind GABA-induced Cl^- fluxes by one sampling point (1 s). This lag is due to the kinetics of Cl^- binding by YFP, which binds Cl^- over a time course of $\sim$100 ms (depending on pH and $[Cl^-]$; Jayaraman et al., 2000). This must be kept in mind when attempting to measure extremely rapid changes in $[Cl^-]$. A second potential problem is that the YFP and CFP fluorophores of Clomeleon can bleach at different rates, which would distort calibration of the indicator signal. Specifically, YFP bleaches faster than CFP (data not shown) and such differential bleaching will cause overestimation of $[Cl^-]_i$ by reducing the emission ratio. In practice, it is not difficult to measure Clomeleon fluorescence at light levels where bleaching is minimal (see Experimental Procedures). Finally, the Cl^- affinity of Clomeleon—approximately 90 mM inside hippocampal neurons (Figure 3C)—is 4- to 10-fold lower than $[Cl^-]_i$, somewhat limiting the response of the indicator around resting $[Cl^-]_i$ levels. This is not a severe problem because our results show that it is even possible to measure declines in $[Cl^-]_i$ (e.g., Figure 5B). Further, this low affinity could also make Clomeleon useful for measuring extracellular $[Cl^-]$, for example, in screening for defective Cl^- fluxes in cystic fibrosis (Kerem et al., 1989). If these properties became limiting for certain applications, systematic mutagenesis of Clomeleon probably could be used to select improved variants.

Even with these limitations, the properties of Clomeleon compare very favorably to those of the organic Cl^- indicators that have been developed (Table 2). Problems common to these quinolinium-derived indicators include toxic loading procedures, poor intracellular retention, excitation with near-UV light, dim fluorescence, and, for most, spectral properties incompatible with ratiometric measurements of absolute $[Cl^-]$. Some indicators circumvent one or another of these problems: for example, MEQ provides better intracellular retention, Lucigenin is excited in the visible spectrum, and MQxyDMAQ allows ratiometric measurements (Table 2). Nonetheless, no organic indicator serves as an optimal solution to all of these problems. Furthermore, most organic indicators are quenched by gluconate, an anion that is often used for electrophysiological recordings. Thus, in almost every respect Clomeleon is preferable over existing indicators for measurements of $[Cl^-]_i$. The organic indicators do, however, have two clear advantages over Clomeleon: most are insensitive to pH changes and respond very rapidly (<1 ms) to changes in $[Cl^-]$.

Since its first application as a reporter for gene expression (Chalfie et al., 1994), GFP has been used in an unprecedented variety of applications, including its use as an indicator for protease activity (Heim and Tsien, 1996), pH (Kneen et al., 1998), and Ca^{2+} (Miyawaki et al., 1997; Romoser et al., 1997). Our results, along with those of Wachter and Remington (1999) and Jayaraman et al. (2000), provide a cautionary note by indicating that applications involving yellow variants of GFP, such as YFP, must take into consideration the effects of halides, NO_3^- and Cd^{2+} on the fluorescence properties of this fluorophore.

Table 2. Cl^- Indicator Properties

Indicator	Ratio-metric	λ_{ex} (nm)	$\epsilon[\phi]$[f]	λ_{em} (nm)	K_d (mM)[j]	F_{max}/F_{min} or R_{max}/R_{min}	pK_a	Halide Selectivity	Sensitivity to Other Anions	Ineffective Anions	Loading and Retention
Clomeleon	yes	440	32,500 [0.4], 94,500 [0.6][d]	485, 527	167[k]	4.8	5.2 (0 Cl^-), 6.5 (150 Cl^-)	$F^- > I^- > Br^- > Cl^-$	NO_3^-	bicarbonate, gluconate	Gene transfer or microinjection; excellent retention
YFP-H148Q[a]	no	514	—	527	140	2.5	7.14 (0 Cl^-), 7.86 (150 Cl^-)	$F^- > I^- > Cl^- > Br^-$	NO_3^-, SCN^-, ClO_4^-, formate	gluconate, SO_4^{2}, PO_4^{2-}, isethionate	Gene transfer or microinjection; excellent retention
MQxyDMAQ[b]	yes	365	5,000 [0.3]	450, 550	10[c,k]	1.33	insens. over pH 6-8	I^-, Br^-	SCN^-	NO_3^-, PO_4^{2-}	Hypotonic shock, reduced form, workable retention, MQ chromophore weakly quenched by proteins
Lucigenin[i]	no	368, 455	36,000, 7,400 [0.6]	505	2.6[c,k]	—	—	$I^- > Br^- > Cl^-$	SCN^-	NO_3^-, PO_4^{2-}, SO_4^{2}	Unstable in cytoplasm, affected by proteins
MEQ[g]	no	344	4,100 [0.7]	440	16–61[c]	—	pH insensitive	I^-, Br^-	SCN^-, gluconate	—	diH-MEQ (oxidized in cell to MEQ), good retention (<10% leakage/h), little photobleaching
ABQ–Dextran[h]	no	345	—	447	6.9	—	—	—	—	—	Microinjection, excellent retention, combined with CI-NERF ratioable (325/450,540)
MQAE[l]	no	355	4,850	460	15[c]	9					Invasive (hypotonic shock), 20% leakage/h
SPQ[e]	no	318, 350	5,430, 3,470 [0.55]	450	83[c]	8	insens over pH 3-10	I^-, Br^-	SCN^-, gluconate, bicarbonate, succinate, citrate, acetate	NO_3^-, PO_4^{2-}	Invasive (hypotonic shock), 2%–10% leakage/h, conditions of rapid leakage possible

[a] Jayaraman et al., 2000
[b] Jayaraman et al., 1999
[c] Reciprocal of Stern-Volmer constant
[d] Values for CFP and YFP from Tsien, 1998
[e] Illsley and Verkman, 1987
[f] ϵ is extinction coefficient (M^{-1} cm^{-1}); ϕ is quantum yield
[g] Biwersi and Verkman, 1991
[h] Biwersi et al., 1992
[i] Biwersi et al., 1994
[j] K_d values determined in situ (unless otherwise indicated)
[k] K_d values determined in vitro
[l] Verkman et al., 1989

Measuring $[Cl^-]$ in Cultured Hippocampal Neurons

Expression of Clomeleon in cultured hippocampal neurons by electroporation resulted in a homogeneously distributed fluorescence signal, an important condition for the measurement of cytoplasmic $[Cl^-]$. Small dendrites and spines were clearly visible, in principle making it possible to investigate highly localized Cl^--based signaling events. Our measurements of resting $[Cl^-]_i$ in cultured hippocampal neurons (7.9 ± 2 mM in pyramidal cells, 20 ± 5 mM in an unselected sample of neurons at P14) compare well with previously published values: 7 mM in hippocampal CA1 pyramidal cells (Staley and Proctor, 1999), 11.4 ± 2.7 mM in cultured rat hippocampal neurons (Hara et al., 1992), and 29.9 ± 4.4 mM (mean Cl^- activity ± SD) in rat sympathetic neurons (Ballanyi and Grafe, 1985). Consistent with the results of Hara et al. (1992), who measured $[Cl^-]_i$ of a bundle of fibers originating from several neurons, we found a slightly higher $[Cl^-]_i$ (25 ± 5.5 mM) in individual peripheral dendrites. Thus, the soma and proximal dendrites of a pyramidal neuron form a single $[Cl^-]_i$ compartment, whereas the very peripheral dendrites may form a compartment of higher $[Cl^-]_i$.

Although a developmental switch of GABA-mediated transmission from excitatory to inhibitory has been attributed to a concurrent change in $[Cl^-]_i$ (Cherubini et al., 1991, Rivera et al., 1999), it has not yet been directly documented that $[Cl^-]_i$ changes during development. Here, we show that $[Cl^-]_i$ drops dramatically between developmental stages E18 and P14 (Figure 4). Though we did not measure intracellular pH at all of these ages, it has been reported that the pH of neurons changes very little over development (Bevensee et al., 1996). Thus, the changes we report are likely due to developmental changes in $[Cl^-]_i$ rather than pH. While our measurements were made in cultured neurons, whose developmental processes may deviate from those in vivo, the changes in $[Cl^-]_i$ that we have measured parallel those thought to occur in vivo. Specifically, our results agree well with the predicted changes in E_{Cl} during the first postnatal week (Cherubini et al., 1991). They also echo the temporal pattern of expression of a K^+/Cl^- cotransporter that has been suggested to diminish $[Cl^-]_i$ within the first two postnatal weeks (Rivera et al., 1999). Thus, our results are consistent with the notion that changes in $[Cl^-]_i$ convert GABAergic synaptic inputs from excitatory to inhibitory during development.

Clomeleon also allowed us to measure shifts in $[Cl^-]_i$ resulting from activation of GABA receptors. Simultaneous electrophysiological recordings indicated that GABA-induced currents as small as 100 pA could produce measurable changes in $[Cl^-]_i$. The agreement between changes in $[Cl^-]_i$ predicted from the integral of GABA-activated currents and the measured $[Cl^-]_i$ signals (Figure 5E) as well as the correlation between peak current amplitudes and maximal changes in $[Cl^-]_i$ (Figure 5C) illustrate the fidelity of Clomeleon in reporting $[Cl^-]_i$ transients. Furthermore, intracellular pH remained unchanged during $GABA_A$ receptor–mediated Cl^- influx (Figure 5E), indicating that Clomeleon was reporting only changes in $[Cl^-]_i$.

GABA-induced currents comparable in magnitude to synaptically activated inhibitory postsynaptic currents (Brown and Johnston, 1983; Thompson and Gahwiler, 1989) produced large changes in $[Cl^-]_i$ for both inward and outward Cl^- fluxes (Figures 5A and 5B). Such GABA-activated $[Cl^-]_i$ shifts have been measured previously with Cl^--selective microelectrodes in rat sympathetic neurons (Ballanyi and Grafe, 1985), crayfish muscle fibers and neurons (Kaila, 1994), and cultured mouse oligodendrocytes (Hoppe and Kettenmann, 1989). Our optical measurements in hippocampal neurons reveal that such shifts in $[Cl^-]_i$ outlast the GABA-induced currents by several seconds. Further, these shifts in $[Cl^-]_i$ result in smaller current responses and further shifts in $[Cl^-]_i$ with subsequent activations of $GABA_A$ receptors (data not shown). A use-dependent depression of GABA-mediated inhibition (Wong and Watkins, 1982; McCarren and Alger, 1985; Thompson and Gahwiler, 1989), also referred to as fading (Segal and Barker, 1984; Huguenard and Alger, 1986), has been attributed to dissipation of the Cl^- driving force by Cl^- accumulation (Barker and Ransom, 1978; Huguenard and Alger, 1986; Akaike et al., 1987). Our observations are consistent with such a mechanism, although in unclamped neurons the magnitude of depletion would be less pronounced than that seen under the voltage-clamp conditions used here. We also demonstrated that increases in somatic $[Cl^-]_i$ produced transient increases of $[Cl^-]_i$ in the dendritic arbor (Figure 6). Thus, Cl^- fluxes into one region of a neuron can modify Cl^--based signaling elsewhere in the neuron, and as a consequence, GABAergic synaptic input onto a neighboring region of a dendrite may be transiently interpreted as excitatory. Such diffusing intracellular Cl^- transients may provide a novel mechanism in the electrical computations performed by a neuron, analogous to the passive spread of current during forward and back propagation of action potentials (Stuart and Sakmann, 1994).

In conclusion, Clomeleon holds considerable promise as a genetically encoded, ratiometric indicator of Cl^- in a multitude of cell types. Future applications may include the screening of expression libraries for proteins modifying Cl^- homeostasis, high-throughput screening of drug libraries, recordings of Cl^- at the internal opening of Cl^--selective ion channels, targeted expression in specific tissues, cells, or subcellular compartments, recordings of extracellular $[Cl^-]$ in confined spaces such as the synaptic cleft, and in vivo recordings of $[Cl^-]$ in behaving animals.

Experimental Procedures

Molecular Biology

A variant of the yellow fluorescent protein, topaz fluorescent protein (TFP, [Ormo et al., 1996]: S65G, S72A, K79R, T203Y, H231L; mutations indicate deviations from the sequence of wild-type GFP [Prasher et al., 1992]) was subcloned by PCR from pGFPtpz-N1 (Packard Instrument Company, Meriden, CT) into a vector derived from pQE30 (Qiagen, Chatsworth, CA) with an altered multiple cloning site designed for simple cassette-based generation of fusion proteins (pQE30-MTK; unpublished data). CFP (cyan fluorescent protein: K26R, F64L, S65T, Y66W, N146I, M153T, V163A, N164H, H231L) was subcloned by PCR from pQE9-CFP (kindly provided by R. Y. Tsien, University of California, San Diego) into pQE30-MTK. The tandem fusion construct (the C terminus of CFP linked with a spacer of 24 amino acids to the N terminus of TFP) was obtained by ligating 62 bp complementary oligonucleotides (CCGGTAGTGG CAGTGGTGAGAATTTGTACTTCCAAGGAGGCGGCAGCGGAG GCA, CTAGTGCCTCCGCTGCCGCCTCCTTGGAAGTACAAATTCTCA

CCACTGCCACTA) with two fragments carrying CFP and TFP resulting in pQE30-Clomeleon. The linker contains a rTEV protease (Life Technologies) cleavage site (ENLYFQG). For CMV-driven expression in cultured hippocampal neurons, an EcI136II–HindIII fragment was subcloned into the mammalian expression vector pRK5 (Schall et al., 1990) cut with SmaI–HindIII. The fusion protein encoded by this construct does not contain the N-terminal MRGSHHHHHHGSA CELGT sequence, and the most C-terminal asparagine residue present in the protein expressed in bacteria. All constructs were sequenced over the entire length of the inserts.

Clomeleon was expressed in *E. coli* (XL1 blue, Stratagene, La Jolla, CA) and its hexahistidine tag was used to purify the protein via Nickel affinity chromatography (Qiagen). The purified protein was >90% pure, as assessed by SDS–PAGE/Coomassie blue staining, and was stored at a concentration of 5–10 μM in a buffer containing 100 mM KCl, 10 mM N-2-hydroxy-ethylpiperazine-N′2-ethane-sulfonic acid (HEPES) adjusted to pH 7.4 with KOH.

All optical measurements of recombinant Clomeleon were performed in a 100 μl quartz cuvette on a Fluoromax fluorometer (Spex Industries, Edison, NJ). Before use, Clomeleon was concentrated and desalted using microcon spin columns (Millipore-Amicon). For measurements of Cl^- sensitivity, 0.5–1 μl of Clomeleon solution was diluted into 120 μl of the test solutions with defined Cl^- concentrations. Solutions were adjusted such that fluorescence counts were 3×10^5 to 3×10^6. Solutions typically contained 20 HEPES, pH 7.4, and the test anion with a total osmolarity of ~320 mmol/kg.

Hippocampal Cell Culture and Gene Transfer

Hippocampi from E16 to P4 Sprague–Dawley rats were dissected and cultured on glass cover slips coated with 500 kDa MW poly-D-lysine (Banker and Cowan, 1977). The culture medium consisted of minimal essential medium (MEM), 5% fetal bovine serum, B-27, and Mito+ serum extender (Collaborative Biomedical) at their suggested concentrations, 3.6 g/l glucose, penicillin/streptomycin (5 U/ml), and 500 μM MEM sodium pyruvate (all reagents Life Technologies, Rockville, MD). Chunks of tissue were treated with papain (25 U/ml, Worthington Biochemical, Lakewood, NJ) for 30–60 min, triturated using pipettes of successively smaller tip diameter, plated at densities of 20,000–50,000 per cover slip, and maintained in a 5% CO_2 humidified atmosphere at 37°C for 7–14 days. Embryonic cultures were prepared using similar procedures as described above, with the following exceptions: HBSS medium supplemented with 7 mM HEPES and 0.3% glucose was used for dissection and trituration until plating. Trypsin (200 U/ml) was used instead of papain. Cultures were maintained in N2 medium (MEM [GIBCO] supplemented with $NaHCO_3$ [26 mM)] glucose [1.2%], pyruvate [0.1 mM], ovalbumin from chicken [1 mg/ml], insulin [5 μg/ml], progesterone [20 nM], putrescin [0.1 mM], and selenium dioxide [30 nM]; all supplements obtained from Sigma).

Neurons (culture day 1–12) were electroporated in the presence of pRK-Clomeleon plasmid DNA via a simplification of the procedure described by Teruel et al. (1999). Briefly, 30 μl DNA solution (100–150 ng/μl) was placed on the coverslip, the electrodes were lowered onto the coverslip, and two voltage pulses (200 V/cm, 50 ms, square pulse) of opposite polarity were applied by a Grass Instruments (Quincy, MA) model S-48 stimulator.

Electrophysiology

GABA-induced currents were recorded from neurons maintained in culture for 7–14 days with an Axoclamp 2B amplifier (Axon Instruments, Foster City, CA) and digitized with a TL-1 interface board (Axon Instruments). Data acquisition and analysis was performed with custom-made programs written in Axobasic (Axon Instruments). The pipette solution contained 150 mM K^+, 140 mM gluconate, 10 mM Cl^-, 5 mM ethyleneglycol-bis(β-aminoethyl ether)-N,N,N′,N′-tetraacetic acid (EGTA), 20 mM HEPES adjusted to pH 7.4 with KOH for recording of GABA-induced currents, and combinations of K-gluconate and KCl at a constant K^+ concentration of 150 mM for calibration experiments. Osmolarity was adjusted to 295 mmol/kg. The extracellular solution consisted of 150 mM NaCl, 2.5 mM KCl, 1 mM $MgCl_2$, 1 mM $CaCl_2$, 10 mM D-glucose, 10 mM HEPES adjusted to pH 7.4 with NaOH; osmolarity was adjusted to 310–320 mmol/kg. Pipettes were pulled from borosilicate glass (OD 1.5 mm, ID 1.1 mm, Sutter Instruments, Novato, CA) and had resistances of 2–5 MΩ in normal recording solutions. GABA (1 mM) was applied locally with a high-resistance pipette positioned close to the soma of the neuron. GABA was ejected from pipettes by 10–50 ms nitrogen pulses (30–50 PSI) using a Picospritzer II (Parker Hannifin). For some experiments, a suction pipette was positioned close to the application pipette to prevent diffusional spread of GABA. The GABA solution contained rhodamine dextran (Molecular Probes) to visualize individual applications.

Optical Measurements of Intracellular Cl^-

Fluorescence microscopy was done on a FS600N upright microscope (Nikon, Melville, NY) using a 40× 0.8 NA water immersion objective and a 100 W mercury lamp (Osram, Germany) as a light source. Neutral density filters were used to limit differential bleaching of the fluorophores (absorbances of 0.6–1.42). Fluorescence was elicited using light pulses of 30 ms duration generated with a Uniblitz shutter (Vincent Associates, Rochester). Excitation light was passed through a 440 ± 10 filter and reflected toward the sample with a dichroic mirror (cut-off 460 nm). Emission was split by a dichroic mirror (cut-off 515 nm) into the donor channel (485 ± 15 nm) and the acceptor channel (530 ± 15 nm). Filter cubes were obtained from Chroma Technology (Brattleboro, VT). Signals were recorded with two photomultiplier tubes (model 814, Photon Technology International, Monmouth Junction, NJ) attached to a C-mounted housing (model D-104, PTI) and digitized with the TL-1 interface. A rectangular region of interest was selected within the emission pathway using an adjustable aperture. All [Cl^-] are given as mean ± SEM, unless stated otherwise.

pH Measurements

BCECF (Molecular Probes, OR) was used to determine intracellular pH. Excitation ratioing was performed at 440 ± 10 nm and 480 ± 10 nm, with an emission filter set to 530 ± 15 nm. Calibrations were carried out by bathing cells loaded with BCECF-AM in KCl solutions with pH values of 7.0, 7.2, 7.4, 7.6, and 7.8 in the presence of 10 μM nigericin (Molecular Probes) following the protocol described by Boyarsky et al. (1988). The average intracellular pH of BCECF-loaded hippocampal neurons was 7.13 ± 0.05 (n = 13, mean ± SEM). For recordings from neurons, BCECF free acid was added to the pipette solution at a concentration of 10–100 μM.

Acknowledgments

We are grateful to D. Gitler, J. Lichtman, and R. Schwartz-Bloom for commenting on the manuscript. We thank Y. Xu and J. Morgan for providing cultured hippocampal neurons, R. Kuner for help with primary embryonic cultures, H. Tokumaru for advice on protein purification, and R. Y. Tsien for providing a plasmid encoding cyan fluorescent protein. Supported by the Feodor-Lynen Program of the Alexander von Humboldt Foundation, the Human Frontiers of Science Organization, and by National Institutes of Health grants NS-21624 and NS-34045.

Received July 11, 2000; revised August 30, 2000.

References

Akaike, N., Inomata, N., and Tokutomi, N. (1987). Contribution of chloride shifts to the fade of gamma-aminobutyric acid-gated currents in frog dorsal root ganglion cells. J. Physiol. (Lond.) *391*, 219–234.

Alger, B.E., and Nicoll, R.A. (1979). GABA-mediated biphasic inhibitory responses in hippocampus. Nature *281*, 315–317.

Amos, B.J., and Richards, C.D. (1996). Intrinsic hydrogen ion buffering in rat CNS neurones maintained in culture. Exp. Physiol. *81*, 261–271.

Ascher, P., Kunze, D., and Neild, T.O. (1976). Chloride distribution in Aplysia neurones. J. Physiol. (Lond.) *256*, 441–464.

Ballanyi, K., and Grafe, P. (1985). An intracellular analysis of gamma-aminobutyric-acid-associated ion movements in rat sympathetic neurones. J. Physiol. (Lond.) *365*, 41–58.

Banker, G.A., and Cowan, W.M. (1977). Rat hippocampal neurons in dispersed cell culture. Brain Res. *126*, 397–442.

Barker, J.L., and Ransom, B.R. (1978). Amino acid pharmacology of mammalian central neurones grown in tissue culture. J. Physiol. (Lond.) *280*, 331–354.

Bekar, L.K., and Walz, W. (1999). Evidence for chloride ions as intracellular messenger substances in astrocytes. J. Neurophysiol. *82*, 248–254.

Bekkers, J.M., Richerson, G.B., and Stevens, C.F. (1990). Origin of variability in quantal size in cultured hippocampal neurons and hippocampal slices. Proc. Natl. Acad. Sci. USA *87*, 5359–5362.

Bevensee, M.O., Cummins, T.R., Haddad, G.G., Boron, W.F., and Boyarsky, G. (1996). pH regulation in single CA1 neurons acutely isolated from the hippocampi of immature and mature rats. J. Physiol. (Lond.) *494*, 315–328.

Biwersi, J., and Verkman, A.S. (1991). Cell-permeable fluorescent indicator for cytosolic chloride. Biochemistry *30*, 7879–7883.

Biwersi, J., Farah, N., Wang, Y.X., Ketcham, R., and Verkman, A.S. (1992). Synthesis of cell-impermeable Cl^-sensitive fluorescent indicators with improved sensitivity and optical properties. Am. J. Physiol. *262*, C242–C250.

Biwersi, J., Tulk, B., and Verkman, A.S. (1994). Long-wavelength chloride-sensitive fluorescent indicators. Anal. Biochem. *219*, 139–143.

Bormann, J., Hamill, O.P., and Sakmann, B. (1987). Mechanism of anion permeation through channels gated by glycine and gamma-aminobutyric acid in mouse cultured spinal neurones. J. Physiol. (Lond.) *385*, 243–286.

Boyarsky, G., Ganz, M.B., Sterzel, R.B., and Boron, W.F. (1988). pH regulation in single glomerular mesangial cells. al. Acid extrusion in absence and presence of HCO3. Am. J. Physiol. *255*, C844–C856.

Bright, G.R., Fisher, G.W., Rogowska, J., and Taylor, D.L. (1989). Fluorescence ratio imaging microscopy. Methods Cell Biol. *30*, 157–192.

Brown, T.H., and Johnston, D. (1983). Voltage-clamp analysis of mossy fiber synaptic input to hippocampal neurons. J. Neurophysiol. *50*, 487–507.

Chalfie, M., Tu, Y., Euskirchen, G., Ward, W.W., and Prasher, D.C. (1994). Green fluorescent protein as a marker for gene expression. Science *263*, 802–805.

Cherubini, E., Gaiarsa, J.L., and Ben-Ari, Y. (1991). GABA: an excitatory transmitter in early postnatal life. Trends Neurosci. *14*, 515–519.

Dallwig, R., Deitmer, J.W., and Backus, K.H. (1999). On the mechanism of GABA-induced currents in cultured rat cortical neurons. Pflugers Arch. *437*, 289–297.

Engblom, A.C., Holopainen, I., and Akerman, K.E. (1991). Ethanol-induced Cl^- flux in rat cerebellar granule cells as measured by a fluorescent probe. Brain Res. *568*, 55–60.

Frech, M.J., Deitmer, J.W., and Backus, K.H. (1999). Intracellular chloride and calcium transients evoked by gamma-aminobutyric acid and glycine in neurons of the rat inferior colliculus. J. Neurobiol. *40*, 386–396.

Hara, M., Inoue, M., Yasukura, T., Ohnishi, S., Mikami, Y., and Inagaki, C. (1992). Uneven distribution of intracellular Cl^- in rat hippocampal neurons. Neurosci. Lett. *143*, 135–138.

Harris, R.A., and Allan, A.M. (1985). Functional coupling of g-aminobutyric acid receptors to chloride channels in brain membranes. Science *228*, 1108–1109.

Heim, R., and Tsien, R.Y. (1996). Engineering green fluorescent protein for improved brightness, longer wavelengths and fluorescence resonance energy transfer. Curr. Biol. *6*, 178–182.

Hoffmann, E.K., and Simonsen, L.O. (1989). Membrane mechanisms in volume and pH regulation in vertebrate cells. Physiol. Rev. *69*, 315–382.

Hoppe, D., and Kettenmann, H. (1989). GABA triggers a Cl^- efflux from cultured mouse oligodendrocytes. Neurosci. Lett. *97*, 334–339.

Huguenard, J.R., and Alger, B.E. (1986). Whole-cell voltage-clamp study of the fading of GABA-activated currents in acutely dissociated hippocampal neurons. J. Neurophysiol. *56*, 1–18.

Illsley, N.P., and Verkman, A.S. (1987). Membrane chloride transport measured using a chloride-sensitive fluorescent probe. Biochemistry *26*, 1215–1219.

Inglefield, J.R., and Schwartz-Bloom, R.D. (1999). Using confocal microscopy and the fluorescent indicator, 6-methoxy-N-ethylquinolinium iodide, to measure changes in intracellular chloride. Methods Enzymol. *307*, 469–481.

Inoue, M., Hara, M., Zeng, X.T., Hirose, T., Ohnishi, S., Yasukura, T., Uriu, T., Omori, K., Minato, A., and Inagaki, C. (1991). An ATP-driven Cl^- pump regulates Cl^- concentrations in rat hippocampal neurons. Neurosci. Lett. *134*, 75–78.

Jayaraman, S., Biwersi, J., and Verkman, A.S. (1999). Synthesis and characterization of dual-wavelength Cl^--sensitive fluorescent indicators for ratio imaging. Am. J. Physiol. *276*, C747–C757.

Jayaraman, S., Haggie, P., Wachter, R.M., Remington, S.J., and Verkman, A.S. (2000). Mechanism and cellular applications of a green fluorescent protein-based halide sensor. J. Biol. Chem. *275*, 6047–6050.

Kaila, K. (1994). Ionic basis of $GABA_A$ receptor channel function in the nervous system. Prog. Neurobiol. *42*, 489–537.

Kaila, K., Rydqvist, B., Pasternack, M., and Voipio, J. (1992). Inward current caused by sodium-dependent uptake of GABA in the crayfish stretch receptor neurone. J. Physiol. (Lond.) *453*, 627–645.

Kerem, B., Rommens, J.M., Buchanan, J.A., Markiewicz, D., Cox, T.K., Chakravarti, A., Buchwald, M., and Tsui, L.C. (1989). Identification of the cystic fibrosis gene: genetic analysis. Science *245*, 1073–1080.

Kneen, M., Farinas, J., Li, Y., and Verkman, A.S. (1998). Green fluorescent protein as a noninvasive intracellular pH indicator. Biophys. J. *74*, 1591–1599.

Koch, M.C., Steinmeyer, K., Lorenz, C., Ricker, K., Wolf, F., Otto, M., Zoll, B., Lehmann-Horn, F., Grzeschik, K.H., and Jentsch, T.J. (1992). The skeletal muscle chloride channel in dominant and recessive human myotonia. Science *257*, 797–800.

Lloyd, S.E., Pearce, S.H., Fisher, S.E., Steinmeyer, K., Schwappach, B., Scheinman, S.J., Harding, B., Bolino, A., Devoto, M., Goodyer, P., et al. (1996). A common molecular basis for three inherited kidney stone diseases. Nature *379*, 445–449.

McCarren, M., and Alger, B.E. (1985). Use-dependent depression of IPSPs in rat hippocampal pyramidal cells in vitro. J. Neurophysiol. *53*, 557–571.

Miyawaki, A., Llopis, J., Heim, R., McCaffery, J.M., Adams, J.A., Ikura, M., and Tsien, R.Y. (1997). Fluorescent indicators for Ca^{2+} based on green fluorescent proteins and calmodulin. Nature *388*, 882–887.

Nakamura, T., Kaneko, H., and Nishida, N. (1997). Direct measurement of the chloride concentration in newt olfactory receptors with the fluorescent probe. Neurosci. Lett. *237*, 5–8.

Neher, E., and Augustine, G.J. (1992). Calcium gradients and buffers in bovine chromaffin cells. J. Physiol. (Lond.) *450*, 273–301.

Ormo, M., Cubitt, A.B., Kallio, K., Gross, L.A., Tsien, R.Y., and Remington, S.J. (1996). Crystal structure of the Aequorea victoria green fluorescent protein. Science *273*, 1392–1395.

Prasher, D.C., Eckenrode, V.K., Ward, W.W., Prendergast, F.G., and Cormier, M.J. (1992). Primary structure of the Aequorea victoria green-fluorescent protein. Gene *111*, 229–233.

Rink, T.J., Tsien, R.Y., and Pozzan, T. (1982). Cytoplasmic pH and free Mg2+ in lymphocytes. J. Cell Biol. *95*, 189–196.

Rivera, C., Voipio, J., Payne, J.A., Ruusuvuori, E., Lahtinen, H., Lamsa, K., Pirvola, U., Saarma, M., and Kaila, K. (1999). The K+/Cl^- co-transporter KCC2 renders GABA hyperpolarizing during neuronal maturation. Nature *397*, 251–255.

Romoser, V.A., Hinkle, P.M., and Persechini, A. (1997). Detection in living cells of Ca2+-dependent changes in the fluorescence emission of an indicator composed of two green fluorescent protein variants linked by a calmodulin-binding sequence. A new class of fluorescent indicators. J. Biol. Chem. *272*, 13270–13274.

Schall, T.J., Lewis, M., Koller, K.J., Lee, A., Rice, G.C., Wong, G.H.W., Gatanaga, T., Granger, G.A., Lentz, R., Raab, H., et al. (1990). Molecular cloning and expression of a receptor for human tumor necrosis factor. *61*, 361–370.

Schwartz, R.D., and Yu, X. (1995). Optical imaging of intracellular chloride in living brain slices. J. Neurosci. Methods *62*, 185–192.

Schwartz, R.D., Jackson, J.A., Wiegert, D., Skolnick, P., and Paul, S.M. (1985). Characterization of barbiturate-stimulated chloride efflux from rat brain synaptoneurosomes. J. Neurosci. *5*, 2963–2970.

Segal, M., and Barker, J.L. (1984). Rat hippocampal neurons in culture: properties of GABA-activated Cl^- ion conductance. J. Neurophysiol. *51*, 500–515.

Shiang, R., Ryan, S.G., Zhu, Y.Z., Hahn, A.F., O'Connell, P., and Wasmuth, J.J. (1993). Mutations in the alpha 1 subunit of the inhibitory glycine receptor cause the dominant neurologic disorder, hyperekplexia. Nat. Genet. *5*, 351–358.

Simon, D.B., Karet, F.E., Hamdan, J.M., DiPietro, A., Sanjad, S.A., and Lifton, R.P. (1996). Bartter's syndrome, hypokalaemic alkalosis with hypercalciuria, is caused by mutations in the Na-K-2Cl cotransporter NKCC2. Nat. Genet. *13*, 183–188.

Staley, K.J., and Proctor, W.R. (1999). Modulation of mammalian dendritic GABA(A) receptor function by the kinetics of Cl^- and $HCO3^-$ transport. J. Physiol. (Lond.) *519*, 693–712.

Staley, K.J., Soldo, B.L., and Proctor, W.R. (1995). Ionic mechanisms of neuronal excitation by inhibitory $GABA_A$ receptors. Science *269*, 977–981.

Stuart, G.J., and Sakmann, B. (1994). Active propagation of somatic action potentials into neocortical pyramidal cell dendrites. Nature *367*, 69–72.

Teruel, M.N., Blanpied, T.A., Shen, K., Augustine, G.J., and Meyer, T. (1999). A versatile microporation technique for the transfection of cultured CNS neurons. J. Neurosci. Methods *93*, 37–48.

Thomas, R.C. (1978). Ion-Sensitive Intracellular Microelectrodes (London: Academic Press).

Thompson, S.M., and Gahwiler, B.H. (1989). Activity-dependent disinhibition. I. Repetitive stimulation reduces IPSP driving force and conductance in the hippocampus in vitro. J. Neurophysiol. *61*, 501–511.

Tsien, R.Y. (1998). The green fluorescent protein. Annu. Rev. Biochem. *67*, 509–544.

Verkman, A.S., Sellers, M.C., Chao, A.C., Leung, T., and Ketcham, R. (1989). Synthesis and characterization of improved chloride-sensitive fluorescent indicators for biological applications. Anal. Biochem. *178*, 355–361.

Wachter, R.M., and Remington, S.J. (1999). Sensitivity of the yellow variant of green fluorescent protein to halides and nitrate. Curr. Biol. *9*, R628–R629.

Wagner, S., Castel, M., Gainer, H., and Yarom, Y. (1997). GABA in the mammalian suprachiasmatic nucleus and its role in diurnal rhythmicity. Nature *387*, 598–603.

Wong, R.K.S., and Watkins, D.J. (1982). Cellular factors influencing GABA response in hippocampal pyramidal cells. J. Neurophysiol. *48*, 938–951.